

Rate-Range for an FH-FSK Acoustic Modem

Nathan Parrish and Sumit Roy
University of Washington
Dept. of Electrical Eng., Box 352500
Seattle WA 98195-2500
{nparrish,sroy}@u.washington.edu

Warren L. J. Fox and Payman Arabshahi
University of Washington
Applied Physics Laboratory, Box 355640
Seattle WA 98105-6698
{warren,payman}@apl.washington.edu

ABSTRACT

Signals transmitted through underwater channels experience attenuation due to dissipation of acoustic energy by spreading as well as by absorption. The path loss due to absorption is found to be highly dependent upon the frequency. Ambient noise, which also greatly affects accurate reception of the signal, is also highly dependent upon frequency. For these reasons, the received SNR cannot be assumed to be constant over wideband acoustic signaling schemes. In this paper we determine the (signaling) rate vs. range curves for a FH-FSK modem considering the frequency selective nature of signal attenuation in an acoustic medium.

Categories and Subject Descriptors: A.1. General: Introductory and Survey, J.2. Computer Applications: Physical Sciences and Engineering.

General Terms: Performance

Keywords

Underwater acoustic networks, acoustic energy absorption, FH-FSK

1. INTRODUCTION

Acoustic modem technology has become an increasingly popular area of research, driven by the desire to deploy networks of underwater sensors and vehicles to act as nodes in an ocean observatory as well as maritime security applications. As described in [1], underwater networks of the future will comprise a variety of nodes: both fixed (e.g. tethered to the sea-bed and surface/sub-surface buoys) and mobile such as the underwater autonomous vehicle (UAV) or Seaglider developed by the Applied Physics Laboratory, U. Washington.

Since Seagliders will be deployed for extended periods of time for data collection, they must operate on a constrained energy budget. This predicated the use of energy efficient communications systems designs at the link and MAC layers. Non-coherent FH-FSK systems are commonly used for this reason as the modulation scheme is known for its robustness. Frequency hopping is employed in the Micro-Modem [2] in order to mitigate the effects of ISI. Underwater channels often have long multi-path delay spreads leading to inter-symbol interference

Permission to make digital or hard copies of all or part of this work for personal or classroom use is granted without fee provided that copies are not made or distributed for profit or commercial advantage and that copies bear this notice and the full citation on the first page. To copy otherwise, or republish, to post on servers or to redistribute to lists, requires prior specific permission and/or a fee.

WUWNet'07, September 14, 2007, Montréal, Québec, Canada.
Copyright 2007 ACM 978-1-59593-736-0/07/0009...\$5.00.

even for modest signaling rates. In order to avoid complex signal processing algorithms, a suitable cycle period for frequency hopping is chosen to allow for channel clearing (i.e. the time between successive transmissions over the same channel exceeds the maximum channel dispersion), therefore mitigating the need for equalization at the receiver.

A key component in the design of any networking topology is the transmission range for any node, defined to be the distance at which a single transmitter can transmit to a single receiver with low probability of error. In typical narrowband signaling, the attenuation of the medium is assumed *constant across the signal bandwidth*; therefore, the transmission range is purely a function of the data rate. However, due to varying absorption rates of acoustic energy, underwater channels are typically frequency selective, i.e. the attenuation is *variable* across the signal bandwidth.

In this paper, we investigate the transmission range of an FH-FSK modem operating at several different rates across three different frequency bands. We derive our results using a Rayleigh fading model with no ISI. Rayleigh fading has been shown to be an accurate model for fully saturated shallow underwater channels [3]. Our results will show that the transmission range depends more significantly upon the frequency band for transmission rather than the data rate.

2. FH-FSK ACOUSTIC MODEM

Non-coherent frequency hopping, frequency shift keying allows for a robust, low-cost physical layer solution that is particularly suited for low rate communications. Frequency hopping divides the useable bandwidth into orthogonal frequency bins. The BFSK modulator hops through the bins in a predetermined hopping pattern, and modulates the data at each hop using binary frequency-shift keying. Frequency hopping can be exploited in a multi-user environment in order to share the available bandwidth by allowing a number of users to transmit simultaneously on different hopping patterns. However, frequency hopping is also exploited in a single-user system, allowing the channel to clear between successive transmissions in the same bin; thereby eliminating ISI at the receiver [4]. Table 1 gives a summary of the frequency hopping characteristics that we will use in our single-user analysis.

We analyze the performance of FH-FSK at four different data rates across three different frequency bands: 7.44 – 12.24 KHz, 12.56 – 17.36 KHz, and 22.8 – 27.6 KHz similar to those in the Micro-modem [2]. These three frequency bands will be denoted as the 9 kHz band, the 14 kHz band, and the 25 kHz band.

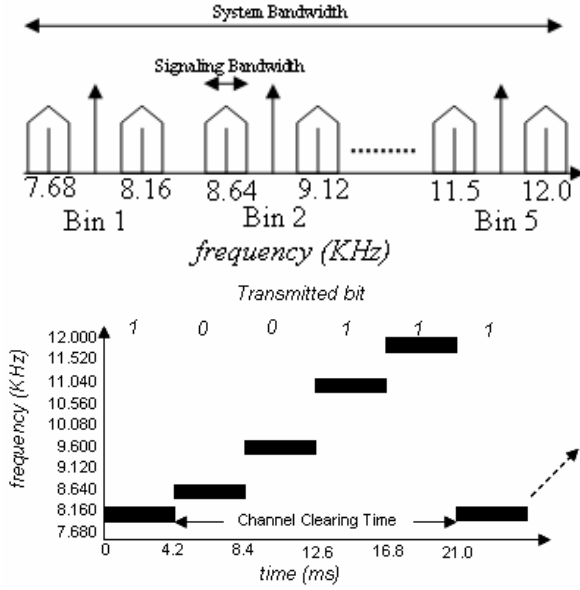


Figure 1. Bandwidth and Hopping Pattern for 240 bps FH-FSK in the 9 kHz band. At each 4.2 ms hop interval, the modulator uses the lower frequency to send a binary 0, or the upper frequency to send a binary 1.

| Frequency Hopping Information | | | | | | |
|-------------------------------|----------------|---------------|------------------|---------------------|--------------------------|--------------------------|
| Data Rate | Number of Bins | Clearing Time | System Bandwidth | Signaling Bandwidth | F _i 9kHz Band | F _h 9kHz Band |
| 80 bps | 13 | 150 msec | 4.160 KHz | 80 Hz | 7.68 kHz | 11.68 kHz |
| 160 bps | 7 | 37.5 msec | 4.480 KHz | 160 Hz | 7.68 kHz | 11.84 kHz |
| 240 bps | 5 | 16.8 msec | 4.800 KHz | 240 Hz | 7.68 kHz | 12 kHz |
| 320 bps | 3 | 6.3 msec | 3.840 KHz | 320 Hz | 8.16 kHz | 11.36 kHz |

Table 1. Characteristics of the FH-FSK Modem. F_i and F_h represent the lowest and upper center frequencies used by the modem for the specific data rate specifically. The 14 kHz and 25 kHz bands are similarly spaced.

3. ACOUSTIC PATH LOSS

The acoustic path loss is given by:

$$A(l, f) = l^k a(f)^l \quad (1)$$

where l is the transmission range in kilometers, k is the spreading factor, and $a(f)$ is the absorption coefficient. The spreading factor is typically between either 1 or 2 for cylindrical and spherical spreading, with 1.5 used as the mean value for many practical scenarios. The absorption coefficient is known experimentally to be a function of several medium factors: the salinity, temperature, depth, pH level etc. The absorption coefficient as a function of frequency is given by the general expression due to Thorp

$$10 \log a(f) = 0.11 \frac{f^2}{1+f^2} + 44 \frac{f^2}{4100+f} + 2.75 \cdot 10^{-4} f^2 + 0.003 \quad (2)$$

where f is in kHz, and $a(f)$ is in dB/km and is valid for frequencies less than 50 kHz. The path loss can thus be written in dB as [5]:

$$10 \log A(l, f) = k \cdot 10 \log(l) + l \cdot 10 \log a(f) \quad (3)$$

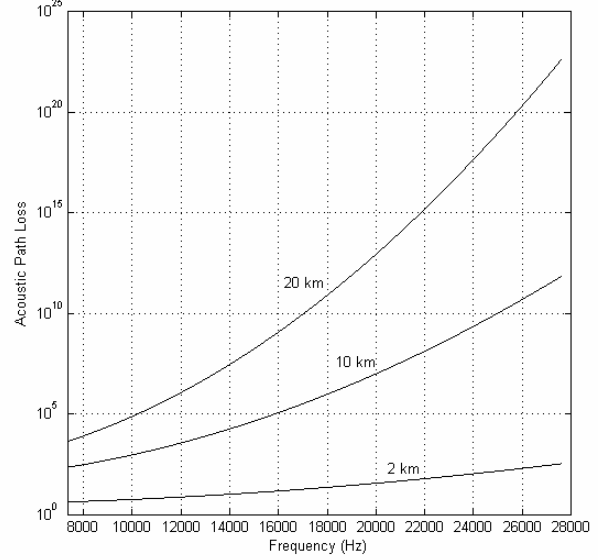


Figure 2. Attenuation vs. frequency at 1 = 2km, 10km, and 20km. It can be seen that for increasing distances, attenuation becomes a log-log function of frequency.

Figure 2 shows the acoustic path loss vs. frequency at three different ranges. As the distance between source and receiver increases, the attenuation becomes more highly dependent upon the frequency.

4. AMBIENT NOISE

Oceanic noise arises from a variety of sources including man-made noise from shipping, thermal noise, turbulence, noise induced by the roughness of the ocean surface, and others. Over the frequency of interest to this study, the ambient noise has been shown to decrease with frequency.

The two primary sources of noise in the 7-25 kHz range are shipping noise and surface agitation. These are given in dB referenced to 1 uPa per Hz by:

$$N_s(f) = 40 + 20 \log(s - 0.5) + 26 \log(f) - 60 \log(f + .03) \quad (4)$$

$$N_w(f) = 50 + 7.5w^{1/2} + 20 \log(f) - 40 \log(f + 0.4) \quad (5)$$

where f is the frequency in kHz, s is the amount of shipping traffic from 0 – 1, and w is the wind speed in meters per second.

An approximation for the total noise power affecting a narrowband signal of bandwidth B hertz is therefore:

$$P_n(f) = 10 \log(10^{N_s(f)/10} + 10^{N_w(f)/10}) + 10 \log(B) \quad (6)$$

where f is the center frequency of the narrowband signal [6].

5. RATE/RANGE CHARACTERIZATION

Given the models for acoustic path loss and ambient noise developed in Sections 3 and 4, we can now derive the relationship between transmission rate and range for the acoustic modem described in Section 2. Under the frequency hopping scenario that we have described, we make the assumption that the channel clearing time will exceed the multi-path delay spread of the channel, and therefore there is no ISI at the receiver. However,

within each transmission we assume narrowband fading. The received signal, neglecting the noise term, is therefore represented as:

$$r(t) = A(l, f)^{-1} \cdot s(t) \left[\sum_{n=0}^{N(t)} \beta_n(t) e^{-j\phi_n(t)} \right] \quad (7)$$

which is the sum of a large number $N(t)$ of unresolved multi-path components of the transmitted signal $s(t)$. Each multi-path signal is affected equally by the attenuation, $A(l, f)$, due to spreading and absorption described in Section 2, and are characterized by $\beta_n(t)$ and $\phi_n(t)$ that represent the random attenuation and phase shift of the n^{th} multi-path component at time t . In the limit of large $N(t)$, the resultant amplitude $\beta(t)$ is well-known to be Rayleigh distributed.

The received *average* SNR is given by

$$\gamma_b = \frac{P_{ref} / A(l, f)}{P_n(f)} \cdot E(\beta^2) \quad (8)$$

where P_{ref} is the reference power in the transmitted signal, $P_n(f)$ is the ambient noise power from Section 4. For non-coherent FSK in Rayleigh fading, the probability of bit error is given by [7]:

$$P(\gamma_b) = \frac{1}{1 + \gamma_b} \quad (9)$$

We use the above results to estimate the probability of error for the acoustic modem under each of its possible operational modes. The modem can transmit at four different symbol rates over 3 different system bands. Additionally, each data rate uses a different number of frequency bins. In Table 2, we compute the value of γ_b for the 160 bps data rate at a range of 10 km in each of the three operating bands of the modem using equation 8. The transmit power is set at 190 dB referenced to 1 μPa , we have assumed practical spreading, and the mean power in the Rayleigh fading coefficient is normalized to 1. We see that average received SNR varies between frequency bins in each system band; specifically in the case of the 25 kHz band, it varies significantly between the FSK frequencies used to transmit a 1 or 0. These different values of received SNR will result in different probabilities of error for each frequency bin, which will be averaged to estimate the overall probability of error for the modem transmitting at a certain data rate within a specified band.

We assume that the probability of transmitting a 1 or 0 is equal and that the modem steps through each bin an equal number of times. Therefore, the probability of error is given by

$$P = \frac{1}{S} \sum_{f=f_1}^{f_s} 0.5 \left(1 + \frac{P_{ref} / A(l, f)}{P_n(f)} \cdot E(\beta^2) \right)^{-1} + 0.5 \left(1 + \frac{P_{ref} / A(l, f + \Delta f)}{P_n(f + \Delta f)} \cdot E(\beta^2) \right)^{-1} \quad (10)$$

where S is the number of frequency bins in the data rate being used, f_x is the frequency used to transmit a binary 0 at bin x , and $f_x + \Delta f$ is the frequency used to transmit a binary 1. Figure 3 shows the probability of error as function of distance. Table 3 summarizes the maximum transmission range if we set the acceptable probability of bit error as 10^{-4} . This table shows that although the maximum transmission range is dependent upon the data rate, it is much more sensitive to the frequency band selected for transmission. Figure 4 shows the final rate/range curves.

| | 9 kHz Band | 14 kHz Band | 25 kHz Band |
|-------|------------|-------------|-------------|
| Bin 1 | 88.779 | 78.763 | 34.414 |
| | 88.423 | 77.851 | 32.542 |
| Bin 2 | 88.028 | 76.906 | 30.640 |
| | 87.596 | 75.930 | 28.710 |
| Bin 3 | 87.126 | 74.922 | 26.751 |
| | 86.619 | 73.882 | 24.764 |
| Bin 4 | 86.076 | 72.812 | 22.748 |
| | 85.498 | 71.710 | 20.703 |
| Bin 5 | 84.885 | 70.578 | 18.630 |
| | 84.237 | 69.415 | 16.529 |
| Bin 6 | 83.555 | 68.221 | 14.399 |
| | 82.840 | 66.997 | 12.240 |
| Bin 7 | 82.090 | 65.742 | 10.054 |
| | 81.308 | 64.457 | 7.838 |

Table 2. Average SNR (dB) in each frequency bin for a modem transmitting at 160 bps. The distance between source and receiver is 10km, noise power is 63 dB re 1 $\mu\text{Pa}/\text{Hz}$, and transmit power is 190 dB re 1 μPa .

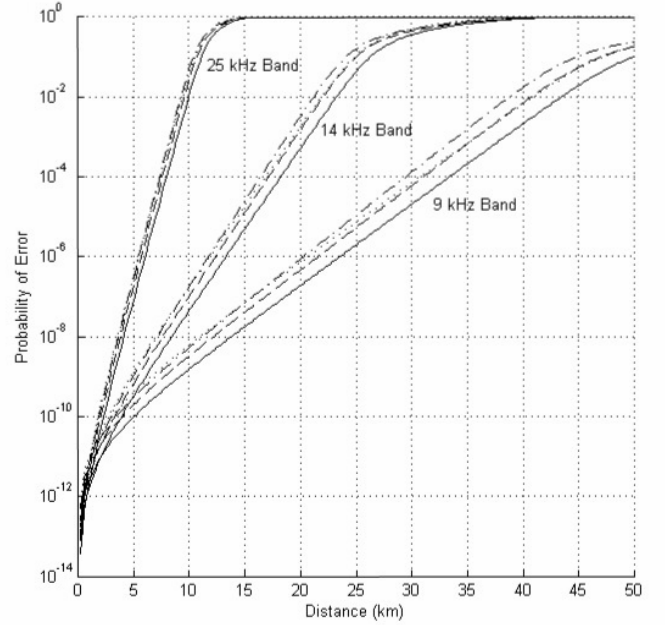


Figure 3. Bit Error Probability for the three frequency bands for 80 bps (solid), 160 bps (dash), 240 bps (dot), 320 bps (dot-dash).

| | 9 kHz Band | 14 kHz Band | 25 kHz Band |
|---------|------------|-------------|-------------|
| 80 bps | 32.0 km | 17.5 km | 7.7 km |
| 160 bps | 29.7 km | 16.5 km | 7.4 km |
| 240 bps | 28.1 km | 15.8 km | 7.1 km |
| 320 bps | 29.3 km | 16.1 km | 7.2 km |

Table 3. Maximum Transmission Range

We can see from Table 3 that the 320 bps signaling rate has a longer range than the 240 bps rate. This is noteworthy as this is not possible in an environment with flat (frequency non-selective)

attenuation and noise across the signaling bandwidth [ie. $A(l,f)$ in (8) is constant and $P_n(f)$ depends only upon the bandwidth]. However, Table 1 shows that the 320 bps signaling scheme uses lower frequencies than the 240 bps scheme. This causes the average absorption coefficient, $a(f)$, across the bins to be lower in the 320 bps scheme. Since attenuation increases exponentially with distance by the absorption coefficient, the 320 bps signaling scheme results in a higher SNR at greater distances despite its higher noise content per bin.

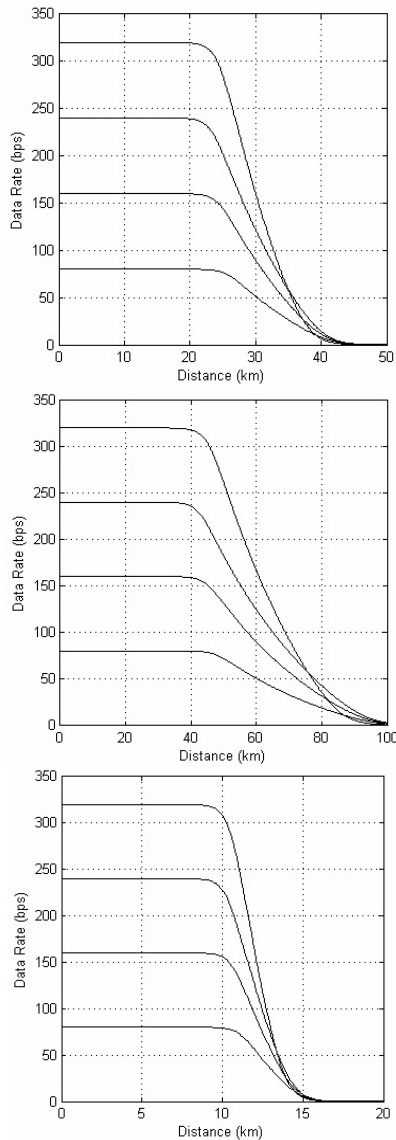


Figure 4. Rate Range Curves for the 9 kHz (top), 14 kHz (middle), and 25 kHz (bottom) bands.

6. CONCLUSIONS and FUTURE WORK

We have shown that the transmission range of a 4 kHz FH-FSK modem is highly dependent upon the frequency bandwidth that the modem occupies. The absorption coefficient of the acoustic medium plays a critical role in determining the received signal power, and thus, the probability of error at the receiver. This will greatly influence the deployment of an underwater network. Nodes that use the 25 kHz bandwidth will need to be spaced densely within an area in order to ensure communication. However, in the 9 kHz band, nodes that are separated by greater distances will have a greater chance of collisions by due to overlap of simultaneous transmissions since the received signal power decays much less slowly with distance.

In future work we intend to verify these results through simulation using a MATLAB model of the WHOI modem provided by Woods Hole Oceanographic Institute and the Sonar Simulation Toolset developed by the Applied Physics Lab at the University of Washington. The Sonar Simulation Toolset provides a detailed acoustics modeling tool that allows the user to specify a range of ocean parameters such as depth, sound speed profile, ambient noise, and surface and bottom characteristics. The results of this analysis will be critical in verifying the assumption of no ISI at the receiver due to the channel clearing time, which will greatly affect the performance of the FH-FSK modem.

7. ACKNOWLEDGEMENT

This work was supported by the NASA Earth Science Technology Office's Advanced Information Systems Technology (AIST) Program under award number AIST-05-0030.

8. REFERENCES

- [1] S. Roy, P. Arabshahi, D. Rouseff and W. L. Fox. Wide Area Ocean Networks: Architecture and System Design Considerations. 1st ACM Workshop on Underwater Networks, Los Angeles, CA, Sep. 2006.
- [2] L. Frietag, M. Grund, S. Singh, J. Partan, P. Koski, K. Balldf. The WHOI Micro-Modem: An Acoustic Communications and Navigation System for Multiple Platforms. In *Proceedings of the IEEE/MTS Oceans Conference*, Washington, DC, USA, September 2005.
- [3] J. Catipovic. Performance Limitations in Underwater Acoustic Telemetry. In *IEEE Journal of Oceanic Engineering*. July 1990, vol. 15, Issue 3. pp. 205-216.
- [4] L. Frietag, M Stojanovic, S Singh, M. Johnson. Analysis of Direct-Sequence and Frequency-Hopped Spread Spectrum Acoustic Communication. In *IEEE Journal of Oceanic Engineering*. October 2001, vol. 26, Issue 4. pp. 586-593.
- [5] M. Stojanovic. On the Relationship Between Capacity and Distance in an Underwater Acoustic Communication Channel. 1st ACM Workshop on Underwater Networks, Los Angeles, CA, September 2006.
- [6] R. Coates. *Underwater Acoustic Systems*. John Wiley & Sons, Inc. New York., 1989.
- [7] J. Proakis. *Digital Communications*. McGraw-Hill, New York, 1995.